Theoretical Calculations of Band Gaps in the Aromatic Structures of Polythieno[3,4-*b*]benzene and Polythieno[3,4-*b*]pyrazine

Ohyun Kwon and Michael L. McKee*

Department of Chemistry, Auburn University, Auburn, Alabama 36849

Received: February 3, 2000; In Final Form: April 14, 2000

Band gaps in polythiophene (**T**) and the related polymers with a fused benzene ring (**TB**, polythieno[3,4-*b*]-benzene) or a fused pyrazine ring (**TN**, polythieno[3,4-*b*]pyrazine) have been computed using a variety of methods. Geometries of oligomers up to octamers (AM1) and up to tetramers (B3LYP/6-31G*) have been optimized, while excitation energies have been computed using ZINDO (INDO/S), configuration interaction singles (CIS), and time-dependent density functional theory (TDDFT). Band gaps have been extrapolated from excitation energies. **T** oligomers are found to have nonplanar geometries, though the planar form is only slightly less stable. **TB** oligomers are found to be nonplanar due to steric repulsion between a hydrogen on the fused benzene ring and the thiophene sulfur, while **TN** oligomers are predicted to be planar. As a result, the band gap in the **TN** polymer is predicted to be smaller than in the **TB** polymer. The aromatic/quinoid character of the **TB** oligomer units is discussed. Extrapolation of DFT HOMO−LUMO energies also gives reasonable band gap predictions.

1. Introduction

Over the past decade, much effort has been devoted to the design of new organic conjugated materials which have very low band gaps without the need of doping.[1] The band gap of simple conjugated organic polymers can be tuned by modifying the nature of the repeat unit and changing the substituents. Among conjugated organic polymers, polythiophene and its derivatives have been most widely studied because of their good environmental stability,[2] small band gaps (∼2.0 eV),[3,4] and easy electrochemical preparations.[1−10]

Polythieno[3,4-*b*]benzene (**TB**) is the first known derivative of polythiophene which has a low band gap (1.0−1.2 eV) without doping.[11−14] **TB** can be described as a thiophene ring to which a benzene ring is fused along the $C_\beta-C_\beta$ bond. In heteroaromatic oligomers, it is known that the nodal pattern of the highest occupied molecular orbital (HOMO) is characteristic of the aromatic form while the nodal pattern of the lowest unoccupied molecular orbital (LUMO) is characteristic of the quinoid form.[15,16] Brédas et al. rationalized that fusion of a benzene ring to thiophene effectively increased the quinoid contribution to the electronic structure, by destabilizing the HOMO and stabilizing the LUMO, which decreases the band gap.[17]

There have been several experimental studies of **TB**,[11−14,18−23] as well as theoretical studies at various levels of theory.[17,24−35] A key question in these studies is whether the electronic nature of the **TB** oligomer ground state is aromatic or quinoid (Figure 1), a point which bears directly on the band gap. These previous computational studies indicated that the band gap of the quinoid form is in good agreement with experiment but not the aromatic form. However, previous calculations at the semiempirical (MNDO), semi-ab-initio (PRDDO), and Hartree−Fock (HF) levels may not accurately describe the geometries of **TB** oligomers. MNDO overestimates inter-ring torsional angles between monomer units in conjugated oligomers, which suggests that the quinoid contribution is underestimated.[24,25,34] However, the quinoid structure can be imposed on the **TB** oligomer by replacing the terminal capping hydrogen with a capping methylene group.

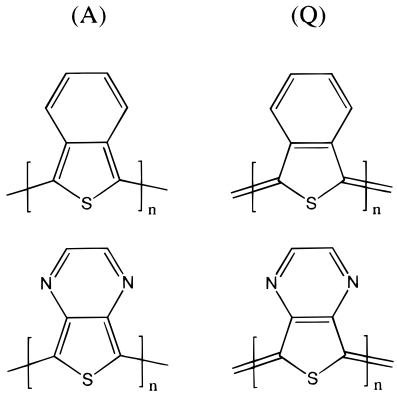

Figure 1. Aromatic (A) and quinoid (Q) structures of polythieno[3,4-*b*]benzene and polythieno[3,4-*b*]pyrazine.

In the **TB** dimer (**TB**2), MNDO produced an almost perpendicular conformation with $\phi = 95°$ between two adjacent rings,[25] while PRDDO gave a dihedral angle of 59°.[26] Brédas first calculated the band structure of **TB** using MNDO-optimized geometries corresponding to the aromatic form, but the calculated band gap was too small (0.54 eV, MNDO; 1.0−1.2 eV, exptl).[17] Lee and Kertesz used MNDO geometries and applied Hückel theory for band structure calculations to both aromatic and quinoid forms of **TB** oligomers.[24,25] The band gaps for the aromatic form (H in the α position of terminal units) and quinoid form (CH_2 in the α position of terminal units) are 0.73 and 1.16 eV, respectively. The band gap of the quinoid form is very close to the experiment, but as mentioned above, the quinoid contribution may be exaggerated by using capping CH_2 groups.

Marynick and co-workers[26] used PRDDO to optimize oligomers for **TB** and **TN** (polythieno[3,4-*b*]pyrazine), where **TN** is related to **TB** by replacing two CH groups in the benzene ring with nitrogen atoms.[33,35−40] They suggested that PRDDO described the S- - -H nonbonded interactions better than MNDO.

10.1021/jp000434g CCC: $19.00
Published on Web 07/06/2000

Using extended Hückel theory on PRDDO geometries, band gaps of 1.64 and 0.80 eV were calculated for the aromatic and the quinoid forms, respectively, which bracket the experimental value of 1.0−1.2 eV. Brédas and co-workers investigated the torsional potential of **TB**2 at various levels of theory and showed that the torsional angle (ϕ) at density functional theory[41] is very similar to that at MP2 ($\phi = 50°$ (DFT), 53° (MP2)),[34] while the torsional angle was larger at HF ($\phi = 65°$)[34] and smaller at AM1 ($\phi = 27°$).[30,32]

A new computational study of **TB** was undertaken to see whether higher levels of theory might reveal new insights into the nature of the band gap in the **TB** system. In addition, an investigation of **TN** (isoelectronic to **TB**) was undertaken at the same level of theory since **TN** is known to be a low band gap polymer and has been synthesized with hexyl substituents on the pyrazine ring.[37]

The experimental band gap of **TN** (0.9 eV)[37,38] is lower than that of **TB** (1.0−1.2 eV), presumably because the absence of S- - -H steric interactions leads to planar **TN** oligomers and more extended conjugation. In the following study, we consider only one set of **TB** and **TN** oligomers, those with H in the α position of terminal units. We find that good agreement with experiment can be obtained from higher levels of theory without enhancing the quinoid character by substituting CH_2 in the α position of terminal units. An aromatic contribution to the **TB**/**TN** oligomers is evidenced by significant delocalization within each unit, while a quinoid contribution is evidenced by conjugation between rings and short inter-ring distances.

In the present study, calculations have been made for **TB***n* and **TN***n* oligomers (where n = the number of units) as well as the parent thiophene oligomers (**T***n*) for comparison. Geometries of oligomers have been optimized under the constraint of symmetry (C_{2h}/C_{2v} for planar structures or C_2 for nonplanar structures) at the semiempirical AM1 level[42] and B3LYP/6-31G* level[43] in density functional theory (DFT). Recently, it has been reported that time-dependent density functional theory (TDDFT)[44−47] gives a satisfactory reproduction of the excitation energies,[46,47] and is superior to the configuration interaction singles (CIS) method,[48] which is based on the HF determinant. In addition, the DFT method has successfully been used to study band gaps in conjugated organic polymers where the HOMO−LUMO difference provides a good estimate of the excitation energy.[49−58] While there is some controversy surrounding the interpretation of DFT orbital energies, recently Savin et al.[52] and Stowasser and Hoffmann[56] have shown that the Kohn−Sham orbitals provide excellent excitation energies. Band gaps for infinite chains of **TB** and **TN** have been determined by plotting excitation energies from **TB** and **TN** oligomers against the inverse of the number of monomer units and extrapolating the number of units to infinity.

2. Computational Details

The SPARTAN[59] program has been used for semiempirical AM1[42] calculations, and the GAUSSIAN 98[60] program has been used for DFT (B3LYP/6-31G*), ZINDO (INDO/S),[61] CIS (CIS-HF/6-31G*), and TDDFT (TD-B3LYP/6-31G*) calculations. Oligomers of **TB** and **TN** have been optimized up to octamers at AM1 and up to tetramers at B3LYP/6-31G*. For comparison, the parent thiophene oligomers have also been optimized up to octamers at AM1 and B3LYP/6-31G*. It is noted that oligomers with an even number of monomer units are characterized by C_{2h} symmetry while oligomers with an odd number of rings have C_{2v} symmetry. Excitation energies, calculated using the ZINDO, CIS, and TDDFT methods and extrapolated to polymer values, will be indicated as ZINDO//"method", CIS//"method", and TDDFT//"method", respectively, where "method" is the level of geometry optimization. Excitation energies approximated by HOMO−LUMO differences at the B3LYP/6-31G* level will be indicated as DFT//"method". The dependence of the band gap on the reciprocal number of monomer units ($1/N$) of oligomers is linear[2,62] and is in excellent agreement with experiment.

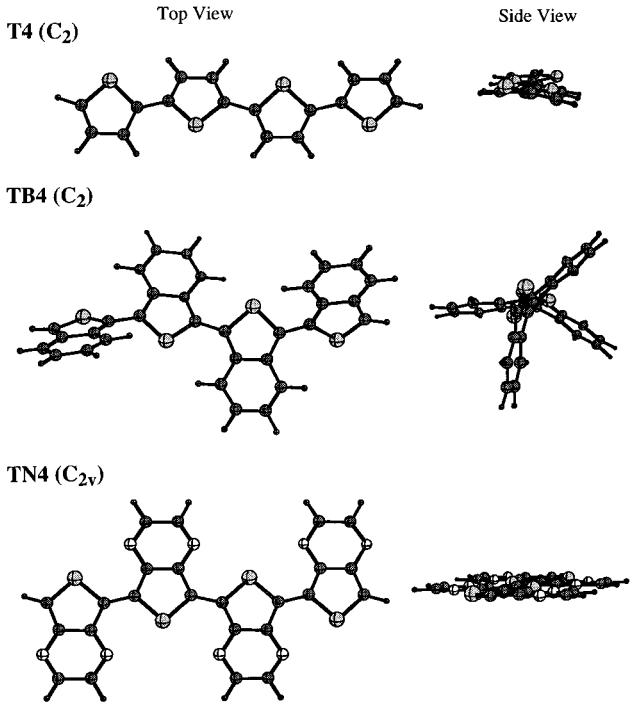

Figure 2. DFT-optimized geometries of tetramers for **T**4, **TB**4, and **TN**4 polymers.

TABLE 1: Calculated Inter-ring C−C Distances (Å) and Ring Torsional Angles (ϕ, deg) for Thiophene (T) at the AM1 and DFT Levels[a]

		C−C (ϕ)	C−C (ϕ)	C−C (ϕ)	C−C (ϕ)
T2	AM1	1.424 (27.9)			
	DFT	1.451 (22.1)			
T3	AM1	1.424 (28.4)			
	DFT	1.448 (16.5)			
T4	AM1	1.424 (28.7)	1.424 (26.3)		
	DFT	1.447 (17.0)	1.444 (14.6)		
T5	AM1	1.424 (23.2)	1.424 (23.0)		
	DFT	1.447 (16.1)	1.442 (7.7)		
T6	AM1	1.424 (26.5)	1.424 (24.4)	1.424 (23.6)	
	DFT	1.446 (14.2)	1.442 (1.2)	1.441 (0.4)	
T7	AM1	1.424 (10.0)	1.423 (10.1)	1.423 (10.0)	
	DFT	1.446 (16.8)	1.442 (7.8)	1.441 (4.4)	
T8	AM1	1.423 (10.0)	1.423 (9.9)	1.423 (10.0)	1.424 (9.9)
	DFT	1.447 (16.2)	1.442 (10.8)	1.441 (4.9)	1.440 (1.4)

[a] The values in each row are C−C inter-ring distances and ring torsional angles from the end to the center of the oligomer. Only the symmetry-unique values are given.

3. Results and Discussions

In Figure 2, we show only the optimized geometries of tetramers of the polythiophene (**T**4), the polythieno[3,4-*b*]-benzene (**TB**4), and the polythieno[3,4-*b*]pyrazine (**TN**4) at the B3LYP/6-31G* level. Calculated C−C bond distances between monomer units and ring torsional angles of oligomers are shown in Tables 1−3. For **T***n*, the nonplanar conformation (C_2 symmetry) is more stable than the planar conformation (C_{2h}/

TABLE 2: Calculated Inter-ring C−C Distances (Å) and Ring Torsional Angles (ϕ; deg) for TB at the AM1 and DFT Levels[a]

		C−C (ϕ)	C−C (ϕ)	C−C (ϕ)	C−C (ϕ)
TB2	AM1	1.422 (26.1)			
	DFT	1.450 (46.0)			
TB3	AM1	1.421 (22.7)			
	DFT	1.447 (42.8)			
TB4	AM1	1.420 (26.3)	1.421 (26.6)		
	DFT	1.446 (42.2)	1.444 (39.8)		
TB5	AM1	1.420 (22.4)	1.420 (20.2)		
TB6	AM1	1.420 (29.6)	1.420 (30.3)	1.421 (30.2)	
TB7	AM1	1.420 (23.8)	1.420 (10.4)	1.420 (11.9)	
TB8	AM1	1.420 (27.3)	1.420 (12.8)	1.420 (13.4)	1.419 (10.9)

[a] The values in each row are C−C inter-ring distances and ring torsional angles from the end to the center of the oligomer. Only the symmetry-unique values are given.

TABLE 3: Calculated Inter-ring C−C Distances (Å) for TN at the AM1 and DFT Levels[a]

		C−C	C−C	C−C	C−C
TN2	AM1	1.419			
	DFT	1.434			
TN3	AM1	1.420			
	DFT	1.429			
TN4	AM1	1.420	1.421		
	DFT	1.426	1.420		
TN5	AM1	1.419	1.420		
TN6	AM1	1.421	1.421	1.420	
TN7	AM1	1.419	1.421	1.420	
TN8	AM1	1.420	1.420	1.420	1.420

[a] The values in each row are C−C inter-ring distances and ring torsional angles from the end to the center of the oligomer. Only the symmetry-unique values are given.

TABLE 4: Relaxation Energies (kcal/mol) for Distortion from the Planar C_{2v}/C_{2h} Structure to the C_2 Structure for T and TB Oligomers (T*n*/TB*n*)

	T*n*		**TB***n*	
n	AM1	DFT	AM1	DFT
2	−0.04	−0.10	−0.35	−3.19
3	−0.07	−0.04	−0.79	−6.02
4	−0.12	−0.09	−1.30	−8.40
5	−0.15	−0.03	−1.65	
6	−0.20	−0.05	−2.12	
7	−0.07	−0.06	−1.52	
8	−0.09	−0.05	−1.95	

C_{2v}) by less than 0.2 kcal/mol at AM1 and B3LYP/6-31G* (Table 4). In general, crystalline oligothiophenes are found to be nearly planar as a result of more favorable crystal packing.[6,63−65] The DFT-optimized geometries are in excellent agreement with the solid-state structure.[64,65] Calculated C−C inter-ring distances (∼1.45 Å) and C−S distances (∼1.75 Å) at the B3LYP/6-31G* are almost equal to experiment (C−C, 1.45 Å; C−S, 1.74 Å), while AM1-calculated distances (C−C, ∼1.42 Å; C−S, 1.68 Å) are somewhat shorter than experiment due to the nature of the AM1 parametrization.[30] It is found that the C−C inter-ring bonds become longer from the center to the end for both AM1 and DFT while the C−S bonds remain constant for both AM1 and DFT.

For thiophene oligomers smaller than pentamer (**T**3, **T**4), the magnitude of the inter-ring torsional angle is similar between all rings (ϕ = 14.6−17.0°). For larger oligomers (**T**5−**T**8), there is a significant reduction in the inter-ring torsional angle in the center of the oligomer compared to the outside. For example, the inter-ring torsional angle in **T**8 (ϕ) is 1.4° at the center and 16.2° at the end (DFT, Table 1).

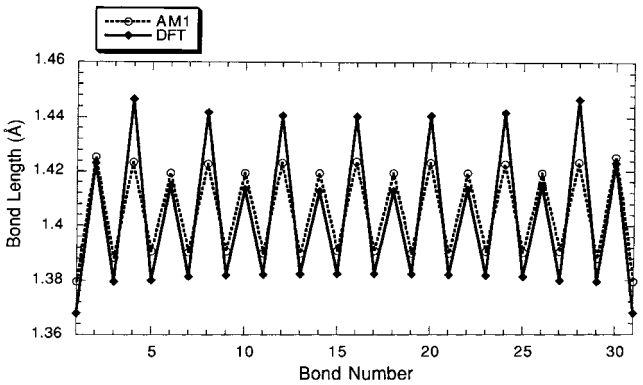

Figure 3. Calculated C−C bond distances of the thiophene octamer (**T**8) at the AM1 and DFT levels.

This suggests that the center rings in the larger thiophene oligomers have more quinoid character than the end rings,[28] which is confirmed by the trends of the C−C bond alternation along the backbone of the thiophene octamer as shown in Figure 3. The C−C bond alternation (Δr) can be defined as the difference between the lengths of a C−C single bond and a double bond. It is observed that Δr for both AM1 and DFT geometries is smaller at the center of the backbone (0.035 and 0.063 Å, respectively) compared to the end (0.037 and 0.068 Å, respectively). Also, it can be noted that there is more bond alternation change in the DFT results (0.063−0.068 Å) compared to AM1 ones (0.035−0.037 Å), which is due to the greater electron delocalization in DFT geometries. Optimized geometries for C_2 symmetry at the DFT level show smaller torsional angles than those at the AM1 level because DFT tends to favor planar over perpendicular conformers.[66] The distances between the β-hydrogen atom and the sulfur atom for the planar conformers (∼2.9 Å, AM1 and DFT) are very close to the sum of van der Waals radii (3.0 Å) of the two atoms.[67] This suggests that there should be minimal steric hindrance between planar thiophene rings at the AM1 and DFT levels. In a comparison of optimized geometries of oligothiophene between AM1 and DFT, DFT geometries are more similar to experiment than AM1 (see above), which suggests that DFT is the preferred method to use in the investigation of polythiophene derivatives such as **TB** and **TN** polymers.

For **TB** oligomers, the energy difference between nonplanar (C_2 symmetry) and planar (C_{2h}/C_{2v}) conformers is larger than in the thiophene oligomers due to the greater steric hindrance between a hydrogen atom of the benzene ring and the sulfur atom in the thiophene ring (S- - -H in planar form, 2.4 Å). The energy difference between planar and nonplanar conformers is about 3 kcal/mol per **TB**−**TB** bond at the DFT level (Table 4), compared to 15 kcal/mol at the PRDDO level and 9 kcal/mol at the HF/STO-3G level.[26] From an analysis of the optical absorption spectra in *n*-hexane solution, Brédas and co-workers reported[32] that **TB** oligomers (with H as the terminal capping group) adopt nonplanar conformations. On the other hand, optimized **TN** oligomers with H as the terminal capping group have only planar conformations because nitrogen (compared to CH in the fused ring) has less steric repulsion with sulfur.

Since there are no experimental structural data for **TB** and **TN** oligomers, we compare our oligomer geometries (**TB***n* and **TN***n*) with those of **T***n*. DFT-calculated C−C inter-ring distances (∼1.44 Å) and C−S distances (∼1.74 Å) for **TB***n* oligomers are not very different from those of the parent thiophene oligomers. We note that C−S bonds are slightly shorter in **TB***n* oligomers than in their thiophene counterparts, which might be related to the existence of a resonance form of

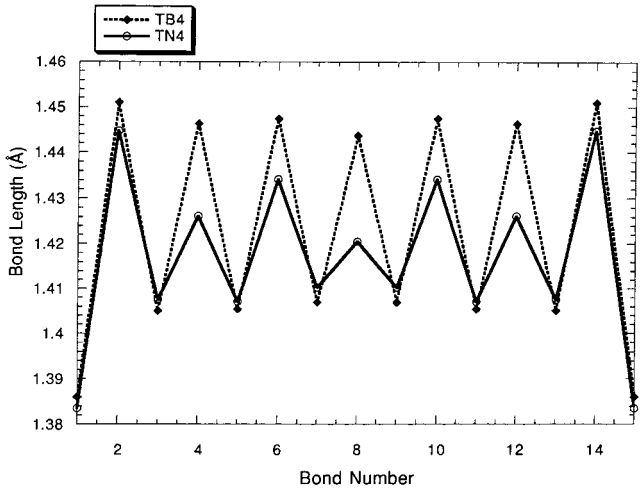

Figure 4. Calculated C−C bond distances of tetramers of **TB** (**TB**4) and **TN** (**TN**4) at the DFT level.

TB oligomers with C−S double bonds. Calculated C−C bond distances in the fused benzene ring explicitly indicate an alternation of single bond and double bond character ($\Delta r \sim 0.05-0.06$ Å), rather than the typical benzene resonance C−C bond distances. Due to the S- - -H nonbonded interactions, the torsional angles are expected to be larger than those in thiophene oligomers. Comparison between optimized tetramers at the DFT level shows **TB**4 and **T**4 have torsional angles of about 40° and 15°, respectively, which can be compared to a torsional angle of 50° from the X-ray structural determination of **TB**2 with bulky substituents (5,5′-bis(*tert*-butyldimethylsilyl)-2,2′-biisothianaphthene).[32] For the planar form of **TB**4, the nonbonded distance between a sulfur atom and a hydrogen atom (S- - -H) is found to be 2.40 Å at the DFT level, compared to 2.83 Å in the nonplanar form.

The geometries of **TN** oligomers are qualitatively different from those of **TB** oligomers. First, all optimized **TN** oligomers are coplanar between monomer units. The unfavorable S- - -H interaction in **TB** is replaced by a S- - -N interaction of 2.98 Å at the DFT level (sum of Van der Waal radii, 3.35 Å),[67] which indicates that steric hindrance between the thiophene ring and the fused pyrazine may not be enough to cause the units to become twisted. Calculated C−C inter-ring distances (∼1.42 Å) for **TN** oligomers at the DFT level are smaller than those for **T** and **TB** oligomers due to greater conjugation through the oligomer backbone in the planar geometry.

By analogy to thiophene oligomers, it is found that the C−C inter-ring distances for **TB** and **TN** oligomers become shorter from the terminal unit to the center unit for both AM1 and DFT, while the C−S bonds change very little for both AM1 and DFT. Also, the AM1 trend of increasing quinoid character (smaller torsional angle at the center of the oligomer) appears when the **TB** and **TN** chain lengths become longer than six units, which is similar to that of **T** oligomers.

The C−C bond alternation of tetramers for the **TB**4 and **TN**4 systems at the DFT level is shown in Figure 4. It is noted that there is more variation in the bond alternation of **TN**4 (0.061−0.010 Å) compared to **TB**4 (0.065−0.037 Å), which can be explained by the fact that the conjugation of **TN**4 is maximized due to planarity. Also, in both **TB**4 and **TN**4, the bond alternation (Δr) at the end of the tetramer (0.065 and 0.061 Å, respectively) is greater than at the center (0.037 and 0.010 Å, respectively).

Extrapolated band gaps are obtained by plotting excitation energies (or HOMO−LUMO differences for B3LYP/6-31G*) from **T**, **TB**, and **TN** oligomer calculations against the inverse number of monomer units and extrapolating to an infinite number of units. In calculating the excitation energies at the ZINDO, CIS, and TDDFT levels, we used the first excited state with significant oscillator strength (a $\pi-\pi^*$ transition), which was also the lowest excited state for all oligomers.

TABLE 5: Calculated Excitation Energies (eV) of the T System (C_2 Symmetry) at the Various Computational Levels

	ZINDO// AM1	ZINDO// DFT	DFT// DFT	CIS// DFT	TDDFT// DFT	exptl[a]	exptl[b]
T2	3.73	3.79	4.35	4.80	4.12		4.10
T3	3.18	3.18	3.55	4.05	3.34		3.49
T4	2.87	2.84	3.13	3.67	2.92		3.18
T5	2.62	2.60	2.84	3.39	2.62		2.98
T6	2.52	2.44	2.64	3.20	2.40		2.87
T7	2.26	2.35	2.53				2.82
T8	2.20	2.28	2.45				
E_g[c]	1.77	1.78	1.82	2.44	1.60	2.0[a]	2.27

[a] Band gap in a thin film.[3,4] [b] Optical band gap in solution. Data from ref 6. [c] E_g corresponds to the extrapolated band gap to an infinite number of units by plotting excitation energies.

Calculated excitation energies (and extrapolated band gaps) for thiophene oligomers at the various theoretical levels based on AM1- and DFT-optimized geometries are shown in Table 5 with the experimental optical band gaps of oligothiophenes up to heptamer.[6] The calculated excitation energies are lower than experiment for each thiophene oligomer. This may be because the experimental values refer to the solution phase, where oligothiophenes are known to be significantly nonplanar ($\phi = \sim 33°$),[68] while the calculated gas-phase geometries have smaller torsional angles (Table 1). The extrapolated optical band gaps of solution-phase oligothiophenes give a band gap of 2.27 eV, which is about 0.3 eV higher than the value obtained in a thin film. The smaller band gap in the thin film is due to the more planar conformers of the oligomers in the solid state. In the discussion below, we compared our calculations with the band gap in a thin film. Brédas has pointed out the relationship between the ring torsional angle and the band gap (smaller torsional angles lead to smaller band gaps).[69]

When excitation energies are extrapolated against the reciprocal number of units, all plots show excellent linearity. However, excitation energies of thiophene heptamer (**T**7) and octamer (**T**8) at the AM1 level deviate somewhat from linearity. This deviation was traced to a dramatic decrease of the ring torsional angles from the hexamer to the heptamer (Table 1, from ∼25° to 10°). In contrast, the DFT torsional angles show a much smoother change from **T**6 to **T**7 to **T**8. The calculated band gap from ZINDO using DFT-optimized geometries is in good agreement with experiment (1.78 eV, ZINDO//DFT; 2.0 eV, exptl). The band gap from extrapolated DFT HOMO−LUMO differences is also in good agreement (1.82 eV, DFT//DFT) with experiment. In particular, extrapolated HOMO−LUMO differences at the B3LYP/6-31G* level are of quality similar to that of a previous study (band gap 2.30 eV) where the B3P86 DFT hybrid functional was specifically modified to improve the agreement between calculated and experimental band gaps.[51]

However, extrapolated CIS excitation energies using DFT-optimized geometries give a band gap too large by about 0.4 eV (Table 5, 2.44 eV, CIS//DFT; 2.0 eV, exptl). TDDFT excitation energies are comparable to those from ZINDO//DFT and experiment, while the extrapolated band gap is underestimated by about 0.4 eV (Table 5). Frisch and co-workers reported that electronic excitation energies for organic molecules are highly sensitive to the choice of the DFT functionals.[47] The

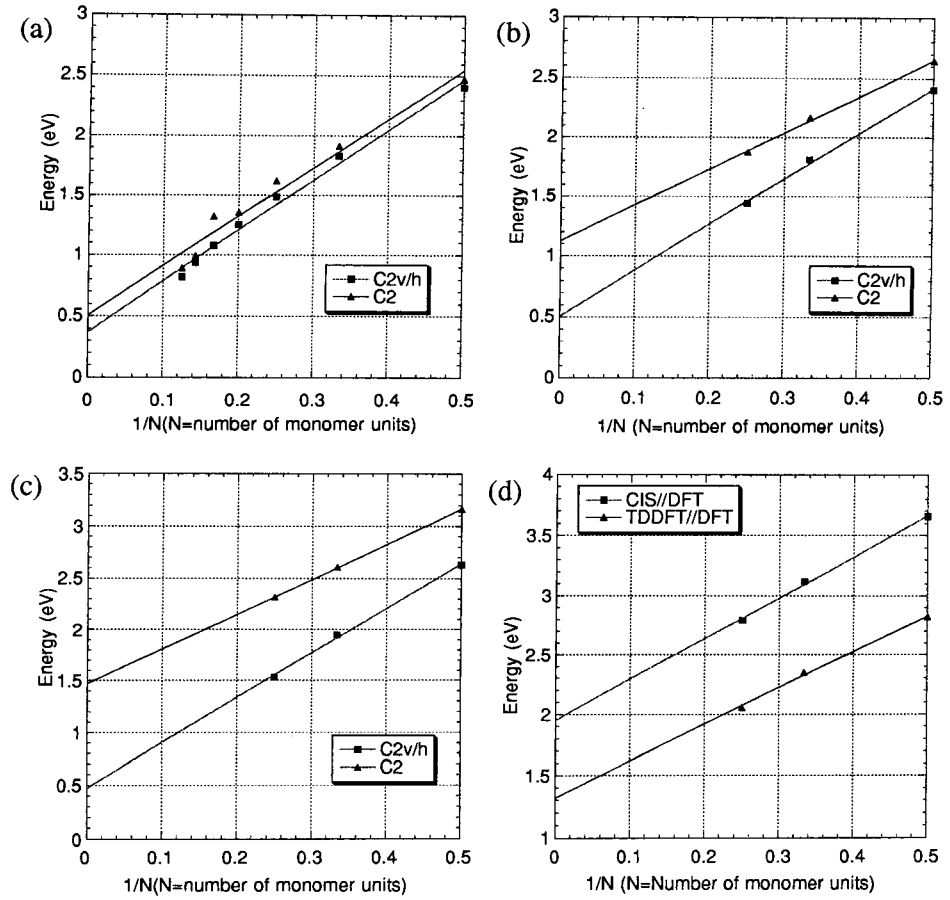

Figure 5. Band gaps extrapolated from plots of excitation energies versus the inverse number of monomer units for **TB** oligomers: (a) ZINDO// AM1, (b) ZINDO//DFT, (c) DFT//DFT, and (d) CIS//DFT and TDDFT//DFT.

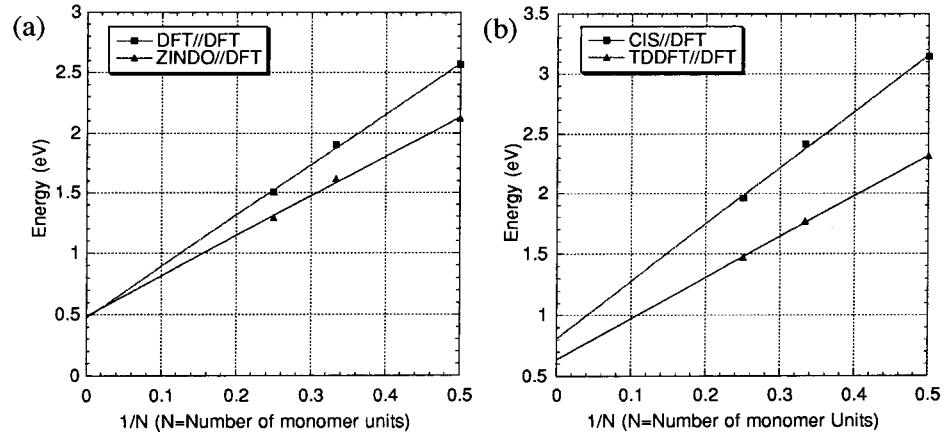

Figure 6. Band gaps extrapolated from plots of excitation energies versus the inverse number of monomer units for **TN** oligomers: (a) ZINDO// DFT and DFT//DFT and (b) CIS//DFT and TDDFT//DFT.

agreement between the theory and experiment is quite satisfactory, especially considering that the experimental measurements were not obtained in the gas phase.

Calculated excitation energies for **TB** and **TN** oligomers are plotted against the inverse number of monomer units and extrapolated to an infinite number of units as shown in Figures 5 and 6, and extrapolated band gaps are summarized in Table 6. For **TB** oligomers, the extrapolated band gaps from ZINDO excitation energies using DFT-optimized geometries are in excellent agreement with the experiment (1.13 eV, ZINDO// DFT; 1.0−1.2 eV, exptl) while AM1-optimized geometries underestimate the band gap by 0.6 eV, which might be due to an underestimation of the ring torsional angle compared to DFT. It is known that the main reason for underestimating band gaps at the semiempirical level is due to neglect of electron correlation.[70] A large change in the torsional angle from the hexamer (**TB**6) to heptamer (**TB**7) at the AM1 level (Table 2) results in a deviation of the calculated excitation energies of **TB**7 and **TB**8 from linearity (a similar deviation was noted above for oligothiophenes). Band gaps from DFT HOMO−LUMO differences are in good agreement with the experiment (1.47 eV, DFT//DFT), which supports the use of DFT HOMO−LUMO differences as predictors of band gaps in organic conjugated polymers. In addition, the TDDFT method reproduces the band gap very well (1.32 eV, TDDFT//DFT) compared to experiment, while the CIS method overestimates the band

TABLE 6: Extrapolated Band Gaps (eV) of T, TB, and TN Oligomers at the Various Computational Levels

	T		TB		TN
	C_2	C_{2v}/C_{2h}	C_2	C_{2v}/C_{2h}	C_{2v}/C_{2h}
ZINDO//AM1	1.77	1.67	0.51	0.37	0.38
ZINDO//DFT	1.78	1.77	1.13	0.51	0.49
DFT//DFT	1.82	1.81	1.47	0.47	0.47
CIS//DFT	2.44	2.44	1.95	0.82	0.81
TDDFT//DFT	1.60	1.59	1.32	0.72	0.64
exptl[a]	2.0[b]		1.0−1.2[c]		0.9[d]

[a] Experimental band gaps are obtained in a thin film. [b] From refs 3 and 4. [c] From refs 11−14. [d] Data from dihexyl-substituted **TN** oligomers.[37,38]

gap (1.95 eV, CIS//DFT) as was also found for the thiophene oligomers. Calculated excitation energies for planar conformers produce smaller band gaps due to the greater conjugation as expected. Our evaluation of band gaps of the **TB** polymer is an improvement from previous theoretical studies (0.73 eV, MNDO; 1.64 eV, PRDDO). In the previous theoretical studies,[24−27] better agreement between the calculated and experimental band gap was obtained when a CH_2 terminal capping group was used, which forces the **TB** oligomer to have a planar quinoid structure. From this agreement, the authors concluded that the **TB** polymer has large quinoid character. It should be pointed out that the current calculations were in very good agreement with the experimental band gap using only hydrogen as the terminal capping group (Table 6). Thus, we suggest that the **TB** polymer may have more aromatic character than hitherto assumed. The large inter-ring torsional angles are predicted to increase the band gap by 0.6 eV compared to the planar form at the ZINDO/DFT and TDDFT//DFT levels (Table 6).

Calculated results of **TN** oligomers show the same trend as found for **T** and **TB** oligomers. The extrapolated band gap from ZINDO//AM1 (0.38 eV) is slightly lower than that from DFT-optimized geometries (ZINDO//DFT, 0.49 eV). The TDDFT//DFT band gap (0.64 eV) is rather close to the ZINDO//DFT and DFT//DFT values, while the CIS//DFT value (0.81 eV) is larger. ZINDO//DFT and DFT//DFT give band gaps of 0.49 and 0.47 eV, respectively (Table 6), which can be compared with the experimental value of 0.9 eV for the dihexyl-substituted **TN** polymer.[37,38] The poorer agreement with experiment could have two origins, both involving the effect of the alkyl substituent. First, the dihexyl substituent could cause the oligomer to become nonplanar, which would reduce the conjugation and increase the band gap.[71] Alternatively, in the dihexyl-substituted **TN** thin film, the long hydrocarbon chains might promote head-to-head aggregation, which would increase the band gap.[6]

A rationalization of the differences in the **T**4, **TB**4, and **TN**4 band gaps can be obtained by comparing DFT HOMO and LUMO orbital energies (Figure 7). The fusion of a benzene ring to a thiophene ring (**T**4 → **TB**4) raises the HOMO by 0.44 eV and lowers the LUMO by 0.38 eV, which is consistent with previous theoretical work.[17,24−35] Since the orbital coefficient at the CH/N position in the HOMO of **TB**4/**TN**4 is about the same as the CH/N coefficient in the LUMO, replacing CH with N will lower the energy of both the HOMO and LUMO by about the same amount. Thus, the HOMO−LUMO difference in **TB**4 (C_{2h}) is about the same as that in **TN**4 (Figure 7, **TB**4/**TN**4, 1.53/1.49 eV). However, when the geometry of **TB**4 is relaxed to C_2, the HOMO energy is stabilized and the LUMO energy is destabilized, giving a HOMO−LUMO difference of 2.31 eV (Figure 7). Therefore, the larger band gap in **TB** compared to **TN** is a direct result of the nonplanar geometry.

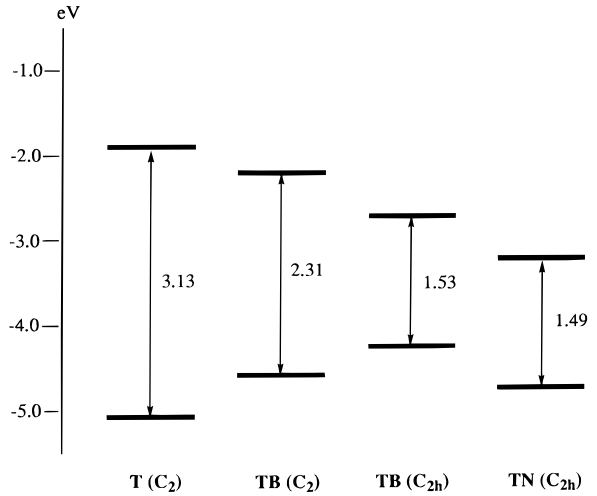

Figure 7. Energy diagram of the HOMO and LUMO of **T** (**T**4), **TB** (**TB**4), and **TN** (**TN**4) systems.

4. Conclusions

Band gaps in **T**, **TB**, and **TN** have been extrapolated from calculated excitation energies of oligomers. While the extrapolation is linear in reciprocal oligomer length, AM1 geometries for the nonplanar heptamer and octamer of **T**, **TB**, and **TN** show a discontinuous change in the ring torsional angles. Several methods were used to determine excitation energies. The ZINDO and TDDFT methods at DFT geometries (ZINDO//DFT and TDDFT//DFT) give results more consistent with experiment, while extrapolation of DFT HOMO−LUMO energy differences was also reasonable. The ZINDO//AM1 method is less consistent due to the use of AM1 geometries, which deviate from DFT results in the predicted degree of conjugation. The CIS//DFT gave band gaps consistently higher than other methods.

The **TB** and **TN** polymers are related to polythiophene by fusing a benzene ring (**TB**) or a pyrazine (**TN**) to the thiophene unit. In the **TB** oligomers (**TB**2−**TB**4) steric repulsion between a benzene hydrogen and sulfur leads to nonplanar geometries where the inter-ring torsional angle is about 40−45° (DFT). In the **TN** oligomers, the CH group is replaced by a nitrogen which reduces the steric repulsion and leads to planar geometries. The larger band gap in **TB** compared to **TN** is a direct result of the nonplanar geometry. Our best predictions (ZINDO//DFT) for the **T**, **TB**, and **TN** band gaps are 1.78, 1.13, and 0.49 eV, respectively, compared to thin-film experimental values of 2.0, 1.0−1.2, and 0.9 eV, respectively.

Good agreement for the band gap of **TB** was obtained with hydrogen as the terminal capping group. Previous theoretical studies used a methylene terminal capping group which exaggerated the quinoid character. Our results suggest that the **TB** oligomer units may have significant aromatic character. Computing DFT HOMO−LUMO energies with different substituents may give a simple way of predicting the substituent effect on polymer band gaps which may be applied to the design of new low band gap oligomers.

Acknowledgment. This work was supported by an EPSCoR grant from the Department of Energy. Computer time was made available on the Alabama Supercomputer Network, at the Maui High Performance Computer Center, and on the HP Exemplar at the University of Kentucky. An equipment grant from Sun Microsystems is acknowledged. We thank Dr. Vince Cammarata for valuable discussions. This paper is dedicated to the memory

of Mike Zerner (1940-2000) in recognition of his contributions to chemistry.

References and Notes

(1) *Handbook of Conducting Polymers*; Skotheim, T. A., Elsenbaumer, R. L., Eds.; Marcel Dekker: New York, 1998.

(2) (a) Schopf, G.; Koβmehl, G. *Polythiophenes—Electrically Conductive Polymers*; Springer-Verlag: New York, 1997. (b) *Handbook of Oligo- and Polythiophenes*; Fichou, D., Ed.; Wiley-VCH: New York, 1999. (c) See contributed chapters: Conjugated Oligomers, Polymers, and Dendrimers: From Polyacetylene to DNA. *Proceedings of the Fourth Francqui Colloquium*, Brussels, October 21-23, 1998; Brédas, J.-L., Ed.; DeBoeck Université: Paris, 1999.

(3) Kobayashi, M.; Chen, J.; Chung, T.-C.; Moraes, F.; Heeger, A. J.; Wudl, F. *Synth. Met.* **1984**, *9*, 77.

(4) Chung, T.-C.; Kaufman, J. H.; Heeger, A. J.; Wudl, F. *Phys. Rev. B* **1984**, *30*, 702.

(5) *Photonic and Optoelectronic Polymers*; Jenekhe, S. A., Wynne, K. J., Eds.; ACS Symposium Series 672; American Chemical Society; Washington, DC, 1997.

(6) *Electronic Materials: The Oligomer Approach*; Müllen, K., Wegner, G., Eds.; Wiley-VCH: Weinheim, 1998.

(7) Yong, C.; Renyuan, R. *Solid State Commun.* **1985**, *54*, 211.

(8) Prasad, P. N.; Swiatkiewicz, J.; Pfleger, J. *Mol. Cryst. Liq. Cryst.* **1988**, *160*, 53.

(9) Sugiyama, T.; Wada, T.; Sasabe, H. *Synth. Met.* **1989**, *28*, C323.

(10) Cava, M. P.; Lakshhmikantham, M. V. *Acc. Chem. Res.* **1975**, *8*, 139.

(11) Wudl, F.; Kobayashi, M.; Heeger, A. J. *J. Org. Chem.* **1984**, *49*, 3382.

(12) Kobayashi, M.; Colaneri, N.; Boysel, M.; Wudl, F.; Heeger, A. J. *J. Chem. Phys.* **1985**, *82*, 5717.

(13) Lazzaroni, R.; Riga, J.; Verbist, J.; Brédas, J. L.; Wudl, F. *J. Chem. Phys.* **1988**, *88*, 4257.

(14) Poplawski, J.; Ehrenfreund, E.; Schaffer, H.; Wudl, F.; Heeger, A. J. *Synth. Met.* **1989**, *28*, C539.

(15) Brédas, J. L.; Thémans, B.; Fripiat, J. G.; André, J. M.; Chance, R. R. *Phys. Rev. B* **1984**, *29*, 6761.

(16) Brédas, J. L.; Chance, R. R.; Silbey, R. *Phys. Rev. B* **1982**, *26*, 5843.

(17) (a) Brédas, J. L.; Heeger, A. L.; Wudl, F. *J. Chem. Phys.* **1986**, *85*, 4673. (b) Brédas, J. L *J. Chem. Phys.* **1985**, *82*, 3808.

(18) Geisselbrecht, J.; Kurti, J.; Kuzmany, H. *Synth. Met.* **1993**, *55*−*57*, 4266.

(19) Kiebooms, R.; Hoogmartens, I.; Adriaensens, P.; Vanderzande, D.; Gelan, J. *Macromolecules* **1995**, *28*, 4961.

(20) Zerbi, G.; Magnoni, M. C.; Hoogmartens, I.; Kiebooms, R.; Carleer, R.; Vanderzande, D.; Gelan, J. *Adv. Mater.* **1995**, *7*, 1027.

(21) Chen, S.-A.; Lee, C.-C. *Pure. Appl. Chem.* **1995**, *67*, 1983.

(22) Chen, S.-A.; Lee, C.-C. *Polymer* **1996**, *37*, 519.

(23) Paulussen, H.; Ottenbourgs, B.; Vanderzande, D.; Adriaensens, P.; Gelan, J. *Polymer* **1997**, *38*, 5221.

(24) Lee, Y. S.; Kertesz, M. *Int. J. Quantum Chem., Quantum Chem. Symp.* **1987**, *21*, 163.

(25) Lee, Y.-S.; Kertesz, M. *J. Chem. Phys.* **1988**, *88*, 2609.

(26) Nayak, K.; Marynick, D. S. *Macromolecules* **1990**, *23*, 2237.

(27) Lee, Y.-S.; Kertesz, M.; Elsenbaumer, R. *Chem. Mater.* **1990**, *2*, 526.

(28) Kürti, J.; Surján, P. R. *J. Chem. Phys.* **1990**, *92*, 3247.

(29) Karpfen, A.; Kertesz, M. *J. Phys. Chem.* **1991**, *95*, 7680.

(30) Hoogmartens, I.; Adriaensens, P.; Vanderzande, D.; Gelan, J.; Quattrocchi, C.; Lazzaroni, R.; Brédas, J. L. *Macromolecules* **1992**, *25*, 7347.

(31) Hong, S. Y.; Marynick, D. S. *Macromolecules* **1992**, *25*, 4652.

(32) Quattrocchi, C.; Lazzaroni, R.; Brédas, J. L.; Kiebooms, R.; Vanderzande, D.; Gelan, J.; Meervelt, L. V. *J. Phys. Chem.* **1995**, *99*, 3932.

(33) Cuff, L.; Kertesz, M. *J. Chem. Phys.* **1997**, *106*, 5541.

(34) Viruela, P. M.; Viruela, R.; Ortí, E.; Brédas, J. L. *J. Am. Chem. Soc.* **1997**, *119*, 1360.

(35) Brocks, G. *J. Phys. Chem.* **1996**, *100*, 17327.

(36) Otto, P.; Ladik, J. *Synth. Met.* **1990**, *36*, 327.

(37) Pomerantz, M.; Chaloner-Gill, B.; Harding, L. O.; Tseng, J. J.; Pomerantz, W. J. *Chem. Commun.* **1992**, 1672.

(38) Pomerantz, M.; Chaloner-Gill, B.; Harding, L. O.; Tseng, J. J.; Pomerantz, W. J. *Synth. Met.* **1993**, *55*, 960.

(39) Kastner, J.; Kuzmany, H.; Vegh, D.; Landl, M.; Cuff, L.; Kertesz, M. *Macromolecules* **1995**, *28*, 2922.

(40) Akoudad, S.; Roncali, J. *Chem. Commun*. **1998**, 2081.

(41) Parr, R. G.; Yang, W. *Density-Functional Theory of Atoms and Molecules*; Oxford University Press: Oxford, 1989.

(42) Dewar, M. J. S.; Zoebisch, E. G.; Healy, E. F.; Stewart, J. J. P. *J. Am. Chem. Soc*. **1985**, *107*, 3902.

(43) Becke, A. D. *J. Chem. Phys.* **1993**, *98*, 5648.

(44) Gross, E. K. U.; Kohn, W. *Adv. Quantum Chem.* **1990**, *21*, 255.

(45) Bauernschmitt, R.; Ahlrichs, R. *Chem. Phys. Lett.* **1998**, *256*, 454.

(46) Casida, M. E.; Jamorski, C.; Casida, K. C.; Salahub, D. R. *J. Chem. Phys*. **1998**, *108*, 4439.

(47) Wiberg, K. B.; Stratmann, R. E.; Frisch, M. J. *Chem. Phys. Lett*. **1998**, *297*, 60.

(48) Foresman, J. B.; Head-Gordon, M.; Pople, J. A.; Frisch, M. J. *J. Phys. Chem.* **1992**, *96*, 135.

(49) (a) Salzner, U.; Lagowski, J. B.; Pickup, P. G.; Poirier, R. A. *J. Comput. Chem*. **1997**, *18*, 1943. (b) Salzner, U.; Pickup, P. G.; Poirier, R. A.; Lagowski, J. B. *J. Phys. Chem. A* **1998**, *102*, 2572.

(50) Salzner, U.; Lagowski, J. B.; Pickup, P. G.; Poirier, R. A. *Synth. Met*. **1998**, *96*, 177.

(51) Salzner, U. *J. Mol. Model.* **2000**, *6*, 195.

(52) Savin, A.; Umrigar, C. J.; Gonze, X. *Chem. Phys. Lett*. **1998**, *288*, 391.

(53) Salzner, U.; Kiziltepe, T. *J. Org. Chem*. **1999**, *64*, 764.

(54) Salzner, U.; Lagowski, J. B.; Pickup, P. G.; Poirier, R. A. *J. Org. Chem*. **1999**, *64*, 7419.

(55) Krzeminski, C.; Delerue, C.; Allan, G.; Haguet, V.; Stiévenard, D.; Frère, P.; Levillain, E.; Roncali, J. *J. Chem. Phys*. **1999**, *111*, 6643.

(56) Stowasser, R.; Hoffmann, R. *J. Am. Chem. Soc*. **1999**, *121*, 3414.

(57) Tozer, D. J.; Amos, R. D.; Handy, N. C.; Roos, B. O.; Serrano-Andrés, L. *Mol. Phys*. **1999**, *97*, 859.

(58) Kwon, O.; McKee, M. L. *J. Phys. Chem. B* **2000**, *104*, 1686.

(59) SPARTAN version 5.0, Wavefunction, Inc., 18401 Von Karman Ave., Suite 370, Irvine, CA 92612.

(60) Frisch, M. J.; Trucks, G. W.; Schlegel, H. B.; Scuseria, G. E.; Robb, M. A.; Cheeseman, J. R.; Zakrzewski, V. G.; Montgomery, Jr., J. A.; Stratmann, R. E.; Burant, J. C.; Dapprich, S.; Millam, J. M.; Daniels, A. D.; Kudin, K. N.; Strain, M. C.; Farkas, O.; Tomasi, J.; Barone, V.; Cossi, M.; Cammi, R.; Mennucci, B.; Pomelli, C.; Adamo, C.; Clifford, S.; Ochterski, J.; Petersson, G. A.; Ayala, P. Y.; Cui, Q.; Morokuma, K.; Malick, D. K.; Rabuck, A. D.; Raghavachari, K.; Foresman, J. B.; Cioslowski, J.; Ortiz, J. V.; Stefanov, B. B.; Liu, G.; Liashenko, A.; Piskorz, P.; Komaromi, I.; Gomperts, R.; Martin, R. L.; Fox, D. J.; Keith, T.; Al-Laham, M. A.; Peng, C. Y.; Nanayakkara, A.; Gonzalez, C.; Challacombe, M.; Gill, P. M. W.; Johnson, B.; Chen, W.; Wong, M. W.; Andres, J. L.; Head-Gordon, M.; Replogle, E. S.; Pople, J. A. *Gaussian 98, Revision A.7*; Gaussian, Inc.: Pittsburgh, PA, 1998.

(61) Zerner, M. C.; Correa de Mello, P.; Hehenberger, M. *Int. J. Quantum Chem*. **1982**, *21*, 251.

(62) (a) André, J.-M.; Delhalle, J.; Brédas, J. L. *Quantum Chemistry Aided Design of Organic Polymers*; World Scientific: River Edge, NJ, 1991. (b) Roncali, J. *Acc. Chem. Res.* **2000**, *33*, 147. (c) Meier, H.; Stalmach, U.; Kolshorn, H. *Acta Polym.* **1997**, *48*, 379.

(63) Hotta, S.; Waragai, K. *J. Mater. Chem*. **1991**, *1*, 835.

(64) Horowitz, G.; Bachet, B.; Yassar, A.; Lang, P.; Demanze, F.; Fave, J.-L.; Garnier, F. *Chem. Mater*. **1995**, *7*, 1337.

(65) Fichou, D.; Bachet, B.; Demanze, F.; Billy, I.; Horowitz, G.; Garnier, F. *Adv. Mater*. **1996**, *8*, 500.

(66) Viruela, P. M.; Viruela, R.; Orti, E. *Int. J. Quantum Chem*. **1998**, *70*, 303.

(67) Huheey, J. E.; Keiter, E. A.; Keiter, R. L. *Inorganic Chemistry*; HarperCollins College Publishers: New York, 1993.

(68) DiCésare, N.; Belletête, M.; Marrano, C.; Leclerc, M.; Durocher, G. *J. Phys. Chem. A* **1998**, *102*, 5142.

(69) Brédas, J. L.; Street, G. B.; Thémans, B.; André, J. M. *J. Chem. Phys*. **1985**, *83*, 1323.

(70) Karelson, M.; Zerner, M. C. *Chem. Phys. Lett.* **1994**, *224*, 213.

(71) When the geometry of **TN**3 was optimized at the AM1 level with two hexyl substituents per unit, the planar form was more stable than the nonplanar form.